World Conference on
Timber Engineering
Oslo 2023

STUDY ON THE MECHANICAL PERFORMANCE OF MULTI-LAYERED BRACKET COMPLEX

Kohei Komatsu[1]

ABSTRACT: This document provides the experimental attempts for making sure the mechanical performance of the multi-layered bracket complex used on the upper parts of stone columns in a repaired ancient temple in China. Making model multi-layered test specimens having layer numbers from 1 to 5, a dynamic vibration test for evaluating the natural frequency and the damping factor was done. Further, using the same test specimens, a push-pull static cyclic loading test was done. It was a satisfactory result that the damping factor of the model multi-layered bracket complex was higher than the preliminary anticipation. Tentative nonlinear analyses using a commercial FEM program on the model multi-layered specimen, however, showed unsatisfactory prediction for the skeleton curves. A lot of further improvements are necessary to do a seismic FEM analysis of the real existing structure involving a multi-layered bracket complex.

KEYWORDS: Multi-layered bracket complex, Damping coefficient, Ancient temple in East Asia

1 INTRODUCTION

In a part of the existing *Kaiyuan* Temple *Tenno-den* (established in 979, largely repaired in 1980) in *Chaozhou* City, *Guangdong* Province, China, the upper part of the stone pillar is composed of the multi-layered bracket complex structure (Figure 1). This structure is a very rare structural form that can only be seen here even in China. This structure is quite motivating for such a researcher who is interested in the structural mechanism of ancient wooden architecture in East Asia. Why was such a multi-layered bracket complex structure adopted? The background and purpose of this research are to scientifically investigate even part of the reason.

Figure 1: *Multi-layered bracket complex structure in Kaiyuan Temple Tenno-den* (*Photo:©Kohei Komatsu*)

[1] Kohei Komatsu, RISH, Kyoto University, Japan
komatsu.kouhei.55z@st.kyoto-u.ac.jp

2 EXPERIMENTS

2.1 SPECIMEN DESIGN

To investigate the mechanical performance of the multi-layered bracket complex structure, a simplified model specimen was created to enable the moment distribution of the actual multi-layered structure shown on the left-hand side[1] of Figure 2 simulate.

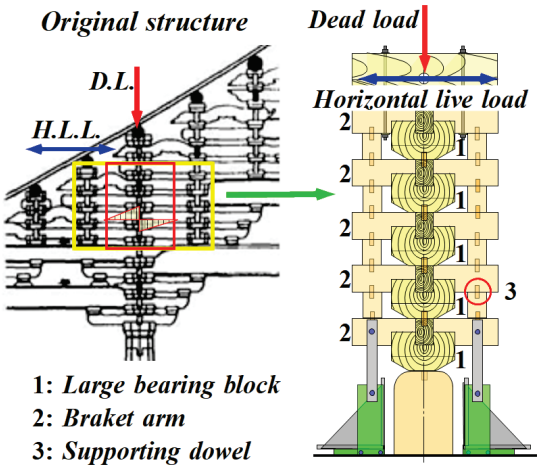

Figure 2: *Simplified model specimen for simulating a part of the actual multi-layered bracket complex structure*[1] *(Refer to Figure16 for the significance of the red-circled #3 dowel when subjected to a tensile force)*

In the yellow square area on the left-hand side of Figure 2, bracket arms are arranged on the large bearing brock

https://doi.org/10.52202/069179-0526

of each layer, and the rotation of the bracket arm is prevented by the vertical dead-load acting on the large bearing brock. This situation can be assumed to be a state in which an anti-symmetrical moment is generated in the bracket arm so as to balance the moment at the large bearing brock, and a zero-moment point in the bracket arm seems to exist around the middle of the two nodes. Therefore, a simplified model multi-layered bracket complex test specimen was proposed as shown in the right-hand side of Figure 2. In this model, the point of zero moment was simulated by setting a pin-joint at both ends of the bracket arm using a supporting wooden block fixed by a dowel.

2.2 KINDS OF MODEL SPECIMEN

To make clear the effect of the number of layers on the mechanical performance of the model specimen, five different kinds of specimens having one to five layers of the bracket complex as shown in Figure 3 were prepared.

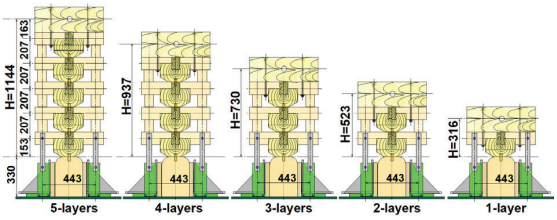

Figure 3: *Five different kinds of model specimens.*

2.3 DYNAMIC TEST SET-UP

To grasp the initial stiffness and damping factor of the model specimens, a sinusoidal sweep vibration test was first conducted by fixing a small exciter on the top of the model specimen as shown in Figure 4.
One accelerometer A_0 was fixed to the steel foundation and another A_1 was fixed to the center of the loading block to measure the response accelerations. At the same time, the horizontal displacement D_1 at the center point of the loading block and the horizontal displacement D_0 at the interface between the bottom of the lowest large bearing block and the column head were measured with displacement measuring devices.

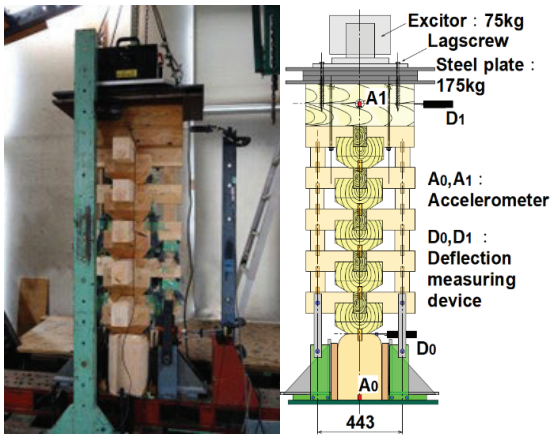

Figure 4: *Test set-up for the dynamic experiment*

The sinusoidal sweep tests were done by giving from 1Hz to 10Hz sin-wave step by step with 1Hz increment to detect the first rough resonance range then the fine sweep-out detections were done with 0.1Hz increment within the range of the first found-out rough region. For this dynamic test, a total of about 2.5 kN weight was loaded, including the weight of the exciter and the steel plates.

2.4 STATIC TEST SET-UP

After finishing the dynamic tests, the static push-pull cyclic horizontal loading tests were conducted using the same test specimens used for the dynamic test.
Figure 5 shows the static test set-up. The vertical dead load was applied on the top of the loading brock using a pulley and wire system which was pulled by an oil jack having 100kN capacity. While the horizontal load was applied at the geometrical center of the loading brock using an oil jack having 250kN capacity.
Horizontal loading protocol was first assigned so as to be set out as the following target values by the shear deformation angle (γ); γ= ±1/300, ±1/200, ±1/150, ±1/100, ±1/75, ±1/60, ±1/50, ±1/40, ±1/30, ±1/20 and ±1/15 rad. Actually, however, in many cases, as the #3 dowel shown in Figure 2 was pulled out when the shear deformation angle was beyond 1/20 rad, thus loading after 1/20 rad was cancelled in such cases. Within each ± target deformation angle, one cycle push-pull loading was given. For the dead load, two loading levels (5kN and 10kN) were adopted.

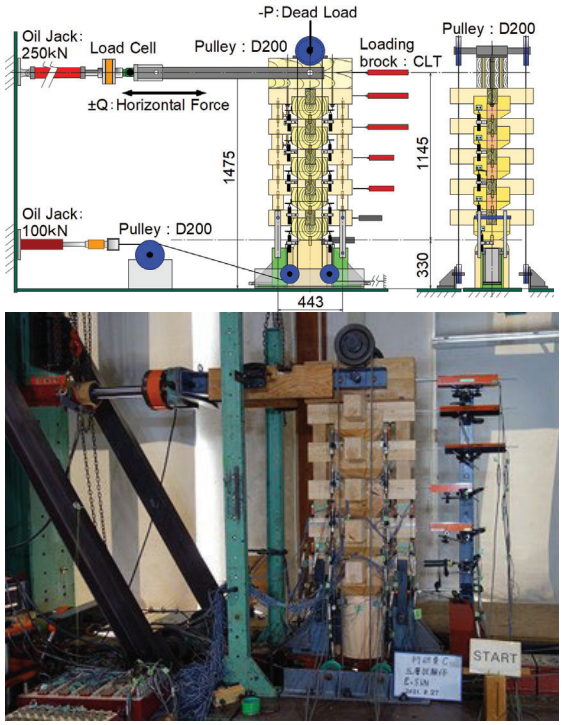

Figure 5: *Test set-up for the static experiment*

https://doi.org/10.52202/069179-0526

2.5 MATERIAL

The test material used was all high-quality solid wood of Japanese cypress (*Chamaecyparis obtusa*) which is preferably used for constructing traditional timber constructions in Japan. The moduli of elasticity of the materials (E0) were measured using an ultrasonic pulse velocity measuring device (PUNDIT-7) as shown in Figure 6. The moisture content was measured using a high-frequency capacitive moisture content meter (Kett HM-520). The result of the mechanical properties of materials is shown in Table 1.

Figure 6: *Measuring E0 using PUNDIT-7*

Table 1:*Mechanical properties of materials used*

	Large bearing brock			Bracket arm		
	ρ*1	MC	E0	ρ*1	MC	E0
	kg/m^3	%	kN/mm^2	kg/m^3	%	kN/mm^2
Mean	471.7	20.9	14.02	472.6	21.9	14.06
STD*2	19.6	1.8	0.95	27.5	3.2	0.83
N	15	15	15	30	30	30

*1:Density
*2:Standard deviation based on the sample number N-1

2.6 ELEMENT TESTS

2.6.1 Dowel shear test

The shear performance of the wooden dowel (d=20mm, L=60mm) joint between the lowest large bearing block and the column head was evaluated by the experiment shown in Figure 7. For the dowel joints belonging to the upper layers than the lowest part, no dowel shear tests were done due to an incorrect judgment of the author.

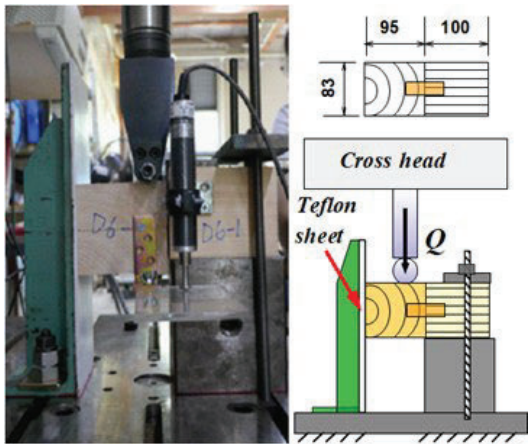

Figure 7: *Shear performance test of wooden dowel joint.*

2.6.2 Moment-resisting test on the large bearing block

To evaluate the quantitative relationship between moment (M) and rotational angle (θ) of the large bearing block, a moment-resisting test shown in Figure 8 was preliminarily done in the elastic stress level using the large bearing blocks which are to be used for the multi-layered bracket complex test specimens.

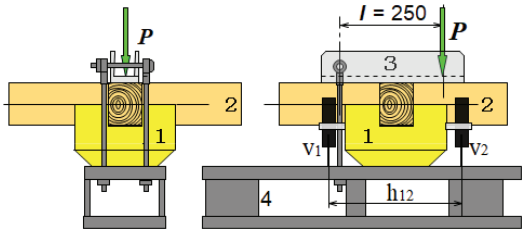

1:Large bearing block (bottom size: 154×154mm)
2:Bracket arm (83×104×571mm)
3:U-shape steel jig
4:Steel base jig

Figure 8: *Moment-resisting test on large bearing block*

In this experiment, moment (M) and rotational angle (θ) were defined by equations (1) and (2).

$$M = P \times 0.25 \quad \text{(kNm)} \tag{1}$$

$$\theta = \frac{v_2 - v_1}{h_{12}} \tag{2}$$

2.6.3 Compressive strength perpendicular to the grain

Compressive strength perpendicular to the grain is an important factor for predicting the yielding performance of the joint between a wooden tie-beam and wooden column according to *Inayama*'s embedment theory [2] and *Kitamori*'s interpretations [3],[4], therefore the compressive strength tests shown in Figure 9 were done using the supporting wood blocks (69×75×102mm) after the main experiments were all finished.

Figure 9 *Compressive strength test of Japanese cypress block perpendicular to the grain.*

3 FINITE ELEMENT MODELING

As a preliminary attempt for predicting the skeleton curve of the multi-layered model specimens provided in this study, FEM analyses using a commercial FEM program were tentatively tried.

https://doi.org/10.52202/069179-0526

3.1 LARGE BEARING BLOCK

The elastic relationship between the moment (M) and the rotational angle (θ) of the large bearing block subjecting to a constant vertical load (P_0) and a moment (M) as shown in Figure 10 was derived based on *Kitamori*'s original proposal [5] as shown in eq. (3).

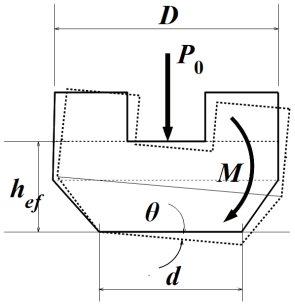

Figure 10: *Definition of the large bearing block subjecting to the moment M and the vertical load P_0*

$$M = \frac{b \cdot d^3 \cdot k_{w90}}{6} \cdot \theta = R_{D1} \cdot \theta \qquad (3)$$

where,

$$k_{w90} = \frac{E_{w90}}{h_{ef}}: \text{ bearing constant (kN/mm}^3) \qquad (4)$$

b: bottom width of the large bearing block (mm)
d: contact length of the large bearing block (mm)
R_{D1}: initial rotational stiffness of the large bearing block
E_{w90}: modulus of elasticity of the large bearing brock perpendicular to the grain estimated as 1/25 of that of the parallel to the grain (E_{w0}) (kN/mm^2)

The first yielding rotational angle was given in equation(5)[5].

$$\theta_{y1} = \frac{2P_0}{b \cdot d^2 \cdot k_{w90}} \qquad (5)$$

The second rotational stiffness was assumed to be smaller than the usual case [2] because the bottom surface of the large bearing block and the upper surface of the bracket arm are both perpendicular to the grain. The second stiffness was assumed as 1/12 of the first stiffness consequently.

$$R_{D2} = R_{D1}/12 \qquad (6)$$

3.2 BRACKET ARM

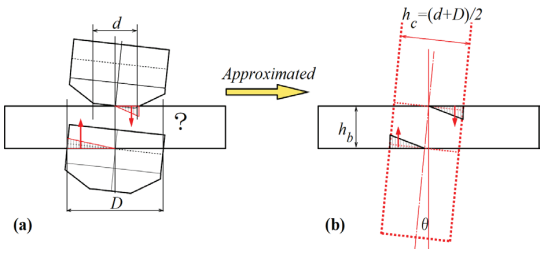

Figure 11: *An approximated mechanical model for the bracket arm contacting with two large bearing blocks.*

Mechanical modelling of the bracket arm seems to be complicated because the equilibrium condition of the vertical resultant forces is unknown as contact areas at the upper and bottom are not the same as shown in Figure 11-(a). Hence, in this study, this situation was approximated by assuming that the pressing condition by the upper and lower large bearing blocks is replaced by that given by a virtual column with an average width $h_c = (d + D)/2$ as shown in Figure 11-(b) and its longitudinal modulus of elasticity is E_{w90}. This assumption implies that the reactions from the virtual column surfaces are far softer than the normal column and tie-beam joint [3] [4] so no spring-back effect nor friction effect will not be considered in this soft contact model.

The moment (M)-rotational angle (θ) relationship for the virtual column-bracket arm joint shown in Figure 11-(b) was derived as equation (7) from *Kitamori* [3].

$$M = \frac{b \cdot {h_c}^3 \cdot k_{w90}}{12} \cdot \theta \qquad (7)$$

where,

b : width of the bracket arm.

$k_{w90} = \frac{E_{w90}}{h_b}$ bearing constant of the bracket arm

The rotational angle at the yielding was given by *Kitamori* [3] [4] as equation (8).

$$\theta_y = \frac{F_m}{h_c k_{w90}\left(1 + \frac{4h_b}{3h_c}\right)} \qquad (8)$$

where,

F_m : bracket arm's partial embedment strength (N/mm^2) =0.8×F_{c90}. In this study, F_{c90} (whole cross-sectional strength) was evaluated by the block compressive test shown in Figure 9.

Figure 12 shows an example of FEM modelling in the case of the three-layered specimen. In this modelling, the large bearing block was simulated by a single spring element having the axial stiffnesses and the rotational stiffness connected with short rigid beams for making the rotational behaviour of the spring element promote.

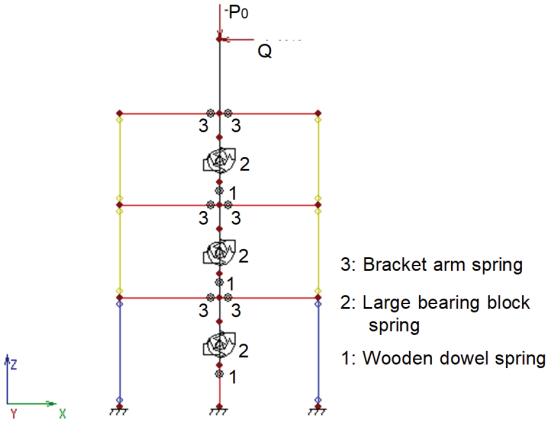

Figure 12: *An example of FEM modelling.*

https://doi.org/10.52202/069179-0526

4 RESULTS AND DISCUSSION

4.1 DOWEL SHEAR TEST RESULTS

Figure 13 shows wood-to-wood doweled shear joint test results. The grain directions of wooden members subject to the shear force were both perpendicular to the grain. While wood-to-wood doweled joints upper than the lowest layer were parallel to perpendicular joints. As no experiments, however, were done for the parallel-to-perpendicular joints, P-Δ curve approximated by a tetra-polygonal line in Figure 13 was applied to all FEM calculations for the multi-layered model specimens.

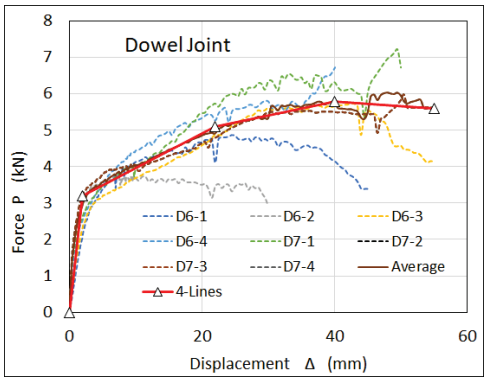

Figure 13: *Dowel joint shear test results and approximation by a tetra-linear polygonal line.*

4.2 VERIFICATION OF THE STIFFNESS OF THE LARGE BEARING BLOCKS

Figure 14 shows comparisons between the observed stiffness and the theoretical one calculated by equation (3) for the large bearing blocks subjecting to the moment shown in Figure 8. Theoretical value seems not to be bad, thus an application of the theoretical stiffness to the FEM models will be appropriate.

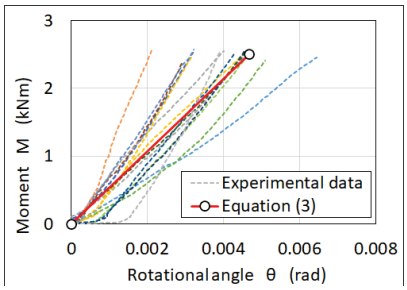

Figure 14: *Comparisons between observed stiffness and theoretical one [eq.(3)] for the large bearing blocks.*

4.3 DYNAMIC TEST RESULTS

In the dynamic test, the natural frequency (*f*) and the damping factor (*h*) of each test specimen were evaluated. The natural frequency (*f*) was evaluated using the Fourie spectral analysis method [e.g. 6]. For the actual calculations, an open computer program SPCANA-Ver4.92 created and provided by Dr. *Teruo Kamada*, an Emeritus Professor at Fukuyama University, was used.

The identification of the damping factor (*h*) was done by the Random Decrement (RD) method [e.g. 7]. For the actual identification, "Random Response Identification Program 3.0.xlsm" created by Dr. *Takehiro Wakita*, former Chubu University, Faculty of Engineering, Department of Architecture, was used.
When using the EXCEL macro, it was important to maintain the condition that the width of the bandpass filter was set so as to include the skirts on either side of the first-order peak of the Fourier spectrum, as described in previous studies [8], [9].

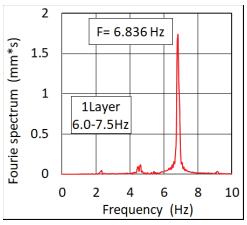

(a)Natural frequency (f)

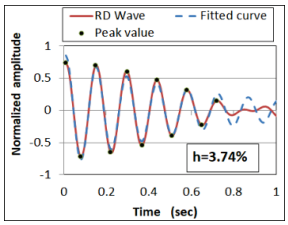

RD method for the 1-layer specimen

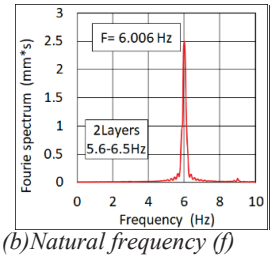

(b)Natural frequency (f)

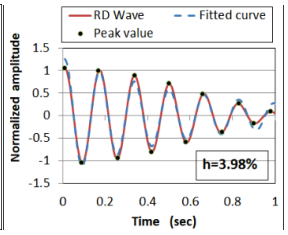

RD method for the 2-layers specimen

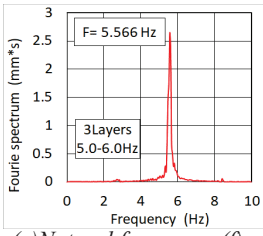

(c)Natural frequency (f)

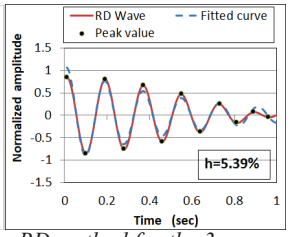

RD method for the 3-layers specimen

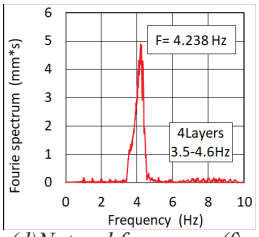

(d)Natural frequency (f)

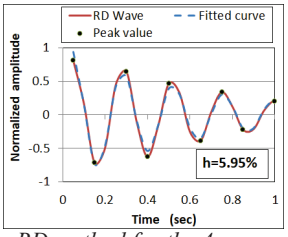

RD method for the 4-layers specimen

https://doi.org/10.52202/069179-0526

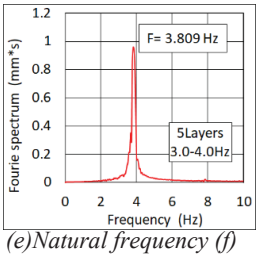

(e)Natural frequency (f)

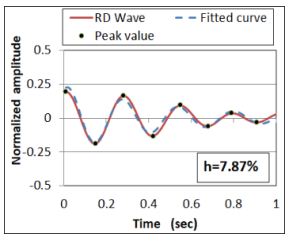

RD method for the 5-layers specimen

Figure 15: *Fourie spectrum and fitting process in the RD method*

Figures 15-(a), (b), (c), (d), and (e) show the identification results of the natural frequency (*f*) by the Fourie spectral analysis method and the fitting process on the selected vibration data of each test specimen for identifying the damping factor (*h*) and the natural frequency (*f*) by the RD method.

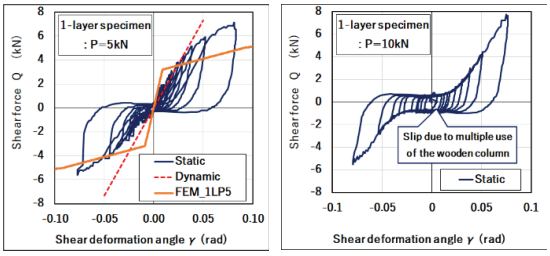

(a)1-Layer Specimen

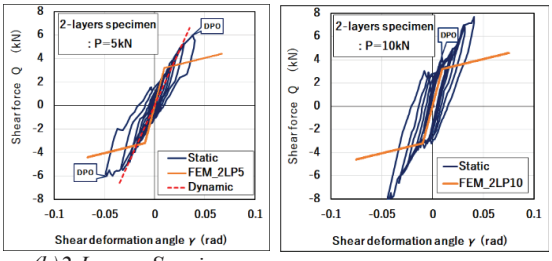

(b)2-Layers Specimen

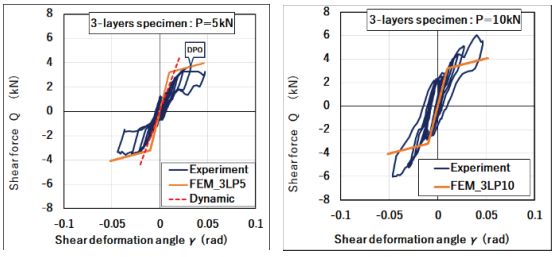

(c)3-Layers Specimen

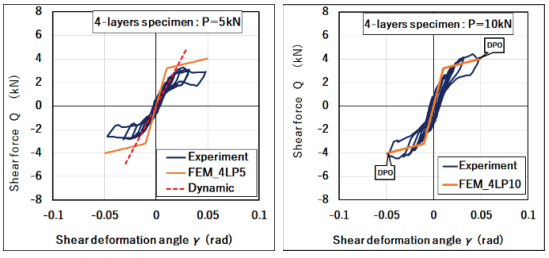

(d)4-Layers Specimen

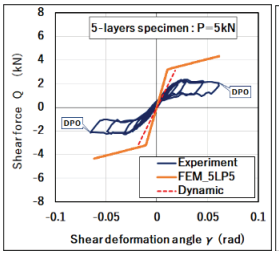

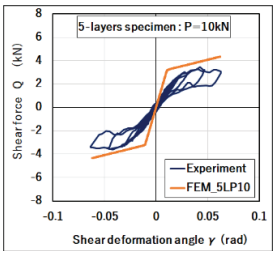

e)5-Layers Specimen

Figure 16: *Shear force Q and shear deformation angle γ relationships of each test specimen.*

**Note: DPO means " pull-out" of #3 dowel shown in Figure 2. This was occurred due to lack of slotted hole at the pin joint in the steel bar for escaping from the tensile force.*

4.4 STATIC TEST RESULTS

The relationships between the shear force Q and the shear deformation angle γ of the test specimens subject to the constant dead load P=5kN and P=10kN are shown in Figure 16-(a), (b), (c), (d) and (e) with FEM analyses results. In the FEM analyses, an optional function for the "*P*Δ-effect" involved in the computer program [10] was used.

The static loading experiments were executed first starting from the 5-layers specimen, next using the same wooden column and a new wooden dowel, 4-layers, 3-layers, 2-layers, and finally 1-layer specimen, therefore in the last specimen (1-layer specimen), large slip occurred as shown in the right-hand side of Figure 16-(a) as the dowel hole became loose due to multiple re-uses of the same column member.

Agreements between the hysteresis curves of the observed Q-γ relationships and predicted skeleton curves by the commercial FEM analysis program were generally bad. One of the reasons for these discrepancies is the unmatured FEM modelling done by the author. Thus, to obtain more satisfactory results, a lot of improvement of the FEM modelling method and reconsiderations on the nonlinear spring constants of each element will be required. While, however, the stiffness (dotted red line) obtained by the dynamic test agreed generally well with the initial slopes of static experimental results.

Figure 17 shows the relationship among the equivalent stiffness (*K*), natural frequency (*f*), damping factor (*h*), and the number of layers of the specimen.

https://doi.org/10.52202/069179-0526

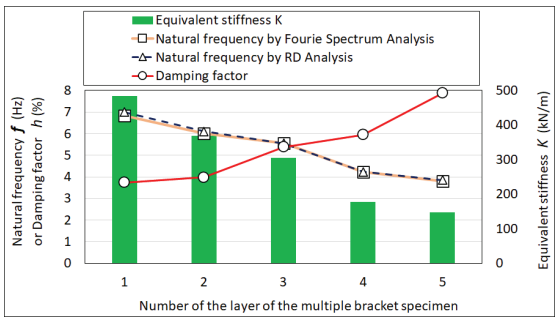

Figure 17: *Relationship among stiffness (K), natural frequency (f), damping factor (h), and number of layers*

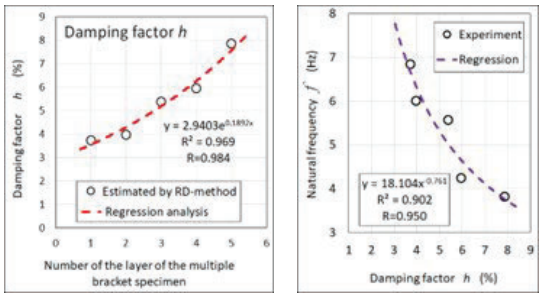

Figure 18: *Relationship among the damping factor (h), number of layers, and the natural frequency (f)*

As can be seen in Figure 17, the evaluated natural frequency (*f*) was considered to be reliable because almost the same values were obtained by both the Fourie Spectral Analysis method and the Random Decrement (RD) method.
There was a tendency for the equivalent stiffness (*K*) that gradually increased as the number of layers of the bracket complex decreased. This tendency seemed to be reasonable judging from the principle of layered structures.
Figure 18 shows the relationship among the damping factor (*h*), the number of layers of the specimen, and the natural frequency (*f*).
As expected preliminary, the damping factor (*h*) increased with the increase of the number of layers as shown in the left-hand side figure of Figure 18. The increasing tendency, however, showed an exponential rather than a linear. In addition, an inversely proportional relationship was observed between the natural frequency (*f*) and the damping factor (*h*) as shown in the right-side hand of Figure 18.

5 CONCLUSION

In this study, a very unique "multi-layered bracket complex structure", which can be seen in *Kaiyuan* Temple *Tenno-den* in *Chaozhou* City, *Guangdong* Province, China, was targeted as the research objective. To clarify at least a small part of the mechanical performance of this unique structure, simplified model layered bracket complex test specimens were created, and dynamic as well as static experimental investigations in conjunction with a tentative FEM modelling composed of beam and spring elements were attempted. Through experimental investigation and numerical analyses, the followings were concluded.

- The model multi-layered test specimens showed an increasing tendency of the damping factor (*h*) as the number of layers increased. This tendency gave an anticipation that this kind of multi-layered structure might have the potential to be a better energy dissipation function.
- Tentative numerical analyses using a commercial FEM program showed unsatisfactory agreements with the hysteresis curves obtained in the static push-pull cyclic loading experiments. Further improvements in the mechanical modelling of each structural element are necessary to obtain more satisfactory results.
- Hysteretic modelling of the multi-layered model specimens has not started yet hence the seismic analyses on the actual temple structure existing in China remained a future research subject.

ACKNOWLEDGEMENTS

This research is funded by the Japan Society for Promoting Science (JSPS) Grant-in-Aid for Scientific Research (C) [No. 21K04352 Principal Investigator: *Kohei Komatsu*].
For executing the experiments, various advice and technical support were given by Mr. *Horimoto Naohiro.* Dr. *Li Zherui*, and Ms. *Zhang Xiaolan* took part in the assistant roles not only for the dynamic and static experiments but also for all the element tests.
The author deeply appreciates not only the financial support from JSPS but also the help and technical support of the above-mentioned three persons.

REFERENCES

[1] *Wu Guozhi*: Architectural Structure of the *Tenno-den* in *Kaiyuan* Temple (1), Ancient Architecture and Garden Technology, 3(16), pp.41-47, 1987. (in Chinese)
[2] *Masahiro Inayama* : Embedment Theory of Timber and Its Application, Ph.D. Thesis Submitted to The University of Tokyo, December, 1991. (in Japanese)
[3] *Akihisa Kitamori*, *Yasuyo Kato*, *Yasuo Kataoka* and *Kohei Komatsu*: "Proposal of mechanical model for beam-column '*nuki*' joint in traditional timber structures", *Mokuzai Gakkaishi* (Journal of the Japan Wood Research Society),49(3), pp.179-186, 2003. (in Japanese)
[4] *Akihisa Kitamori* (Co-author): "4.4 Embedment Theory and *Nuki*-joint", in Fundamental Theory of Timber Engineering, pp.97-103, Architectural Institute of Japan (edited and published), 2010. (in Japanese)
[5] *Akihisa Kitamori, Kiho Jung, Ivon Hassel, Wen-Shao Chang, Kohei Komatsu and Yoshiyuki Suzuki*: Mechanical Analysis of Lateral Loading Behavior on Japanese Traditional Frame Structure Depending

on The Vertical Load, Proceedings of WCTE2010, Italy, 2010.
[6] *Yorihiko Osaki:* New- Introduction to the Spectral Analyses of the Earthquake Motion, *Kajima* Publishing, 1994. (in Japanese)
[7] *John Christian Asmussen*: Modal Analysis Based on the Random Decrement Technique - Application to Civil Engineering Structures, Aalborg: Department of Mechanical Engineering, Aalborg University, 1997. 227 p. (Fracture and Dynamics; No. Paper no. 100). Research output: Book/Report, Ph.D. thesis *https://vbn.aau.dk/en/publications/modal-analysis-based-on-the-random-decrement-technique-applicatio*
[8] *Izuru Okawa, Masanori Iiba, Shin Koyama, Koichi Morita, Shigeki Sakai, Atsushi Fujii, Mitoshi Yasui and Morimasa Watakabe*: Research on Dynamic Characteristics of A Residential Building Based on Micro Tremor Measurement and so on, Building Research Data, No.122, pp.1-51, Building Research Institute, December 2009. (in Japanese)
[9] *Takahiro Toyoda* and *Kiyoshi Takano*: Estimating the Damping Ratio of Buildings Using Weak Seismic Ground Motion: A Case Study on Buildings of the University of Tokyo, Bulletin of the Earthquake Research Institute, The University of Tokyo, Vol.88, pp.1-36, 2013.(in Japanese)
[10] ANON: **S**tructural **N**on-linear **A**nalysis **P**rogram (SNAP) ver.7, Technical Manual, *Kozo* System Inc., 2021. (in Japanese)

https://doi.org/10.52202/069179-0526